

Figure S1. Related to Figure 1. InR and Akt1 temperature control and rescue experiments. (A-D) Flies were maintained at 18°C. (A,C) Representative maximum intensity confocal projections of OR85e axons in the adult antennal lobe region. Four days after axotomy, most GFP+ axonal debris has been cleared. Scale bar = 20 microns. (B,D) Quantification of GFP+ debris after axotomy, normalized to uninjured levels, for experiments shown in A and C, respectively. $N \geq 12$ for each condition and genotype. Mean and SEM plotted. n.s. = not significant. Control (OR85e-mCD8::GFP, tub-Gal80ts/+;repo-Gal4/+), InR/+ Control (OR85e-mCD8::GFP, tub-Gal80ts/+;repo-Gal4, InRex15/+), InRRNAi (OR85e-mCD8::GFP, tub-Gal80ts/+;repo-Gal4, InRex15/UAS-InRRNAi) and dnInR (OR85e-mCD8::GFP, tub-Gal80ts/+;repo-Gal4, InRex15/UAS-Dominant Negative InR) flies, and AktRNAi (OR85e-mCD8::GFP, tub-Gal80ts/+;repo-Gal4/UAS-AktRNAi) (E,G) Representative projections of OR85e axons. (F,H) Quantification of GFP+ debris after axotomy, normalized to uninjured levels, for experiments in E and G, respectively. $N \geq 10$ for each condition and genotype. Mean and SEM plotted. n.s. = not significant. Control (OR85e-mCD8::GFP, tub-Gal80ts/+;repo-Gal4, InRex15/+), InRRNAi (OR85e-mCD8::GFP, tub-Gal80ts/UAS-LacZ::NLS;repo-Gal4, InRex15/UAS-InRRNAi), InRRNAi + InR Rescue (OR85e-mCD8::GFP, tub-Gal80ts/UAS-InR;repo-Gal4, InRex15/UAS-InRRNAi), AktRNAi (OR85e-mCD8::GFP, tub-Gal80ts/UAS-LacZ::NLS;repo-Gal4/UAS-AktRNAi), AktRNAi + Akt Rescue (OR85e-mCD8::GFP, tub-Gal80ts/UAS-Akt1;repo-Gal4/UAS-AktRNAi).

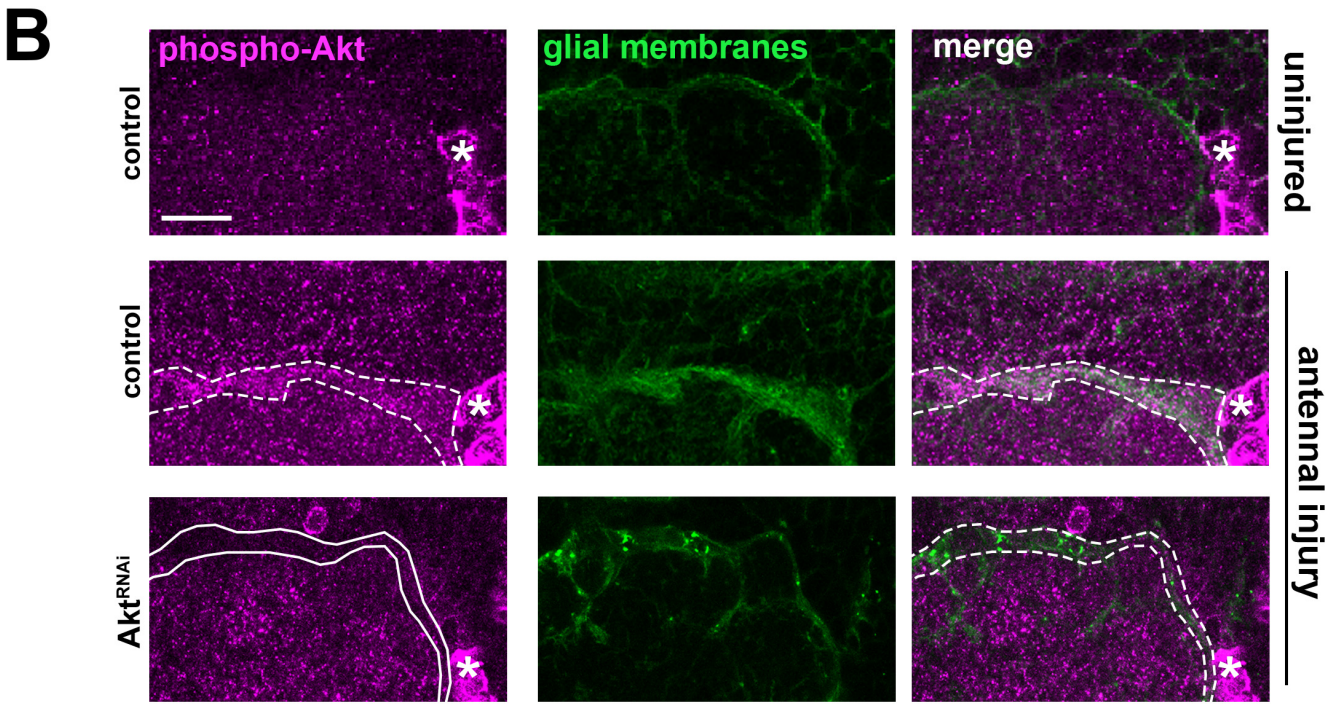
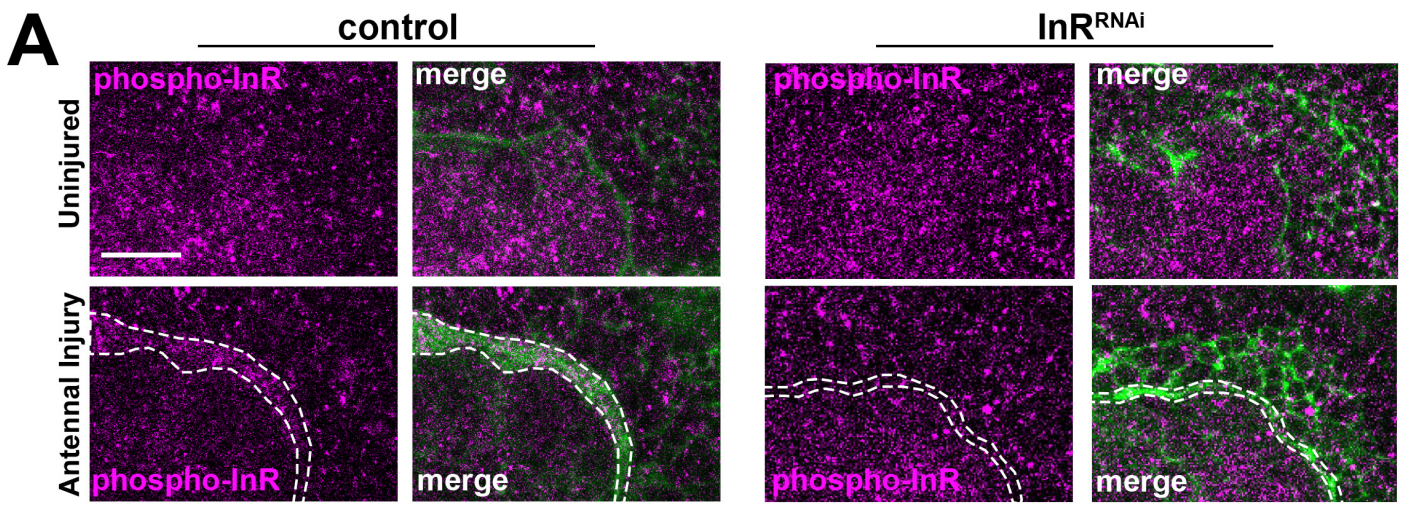


Figure S2. Related to Figure 2. Validation of phospho-InR and phospho-Akt antibody specificity. (A,B) Zoomed confocal images of dorsolateral antennal lobe region shows that increased phospho-InR (A) and phospho-Akt (B) signal in expanding ensheathing glial membranes (green) after antennal nerve axotomy. Injury-induced increases in phospho-InR and phospho-Akt are attenuated when glia are depleted of InR or Akt, respectively. Asterisks denote phospho-Akt signal consistently observed in a subset of neurons adjacent to the antennal lobes. Genotype: control (control (OR85e-mCD8::GFP,tub-Gal80ts/+;repo-Gal4, InRex15/+). InRRNAi (OR85e-mCD8::GFP,tub-Gal80ts/+;repo-Gal4, InRex15/UAS-InRRNAi). AktRNAi (OR85e-mCD8::GFP,tub-Gal80ts/+;repo-Gal4/UAS-AktRNAi). Scale bar = 15 microns.

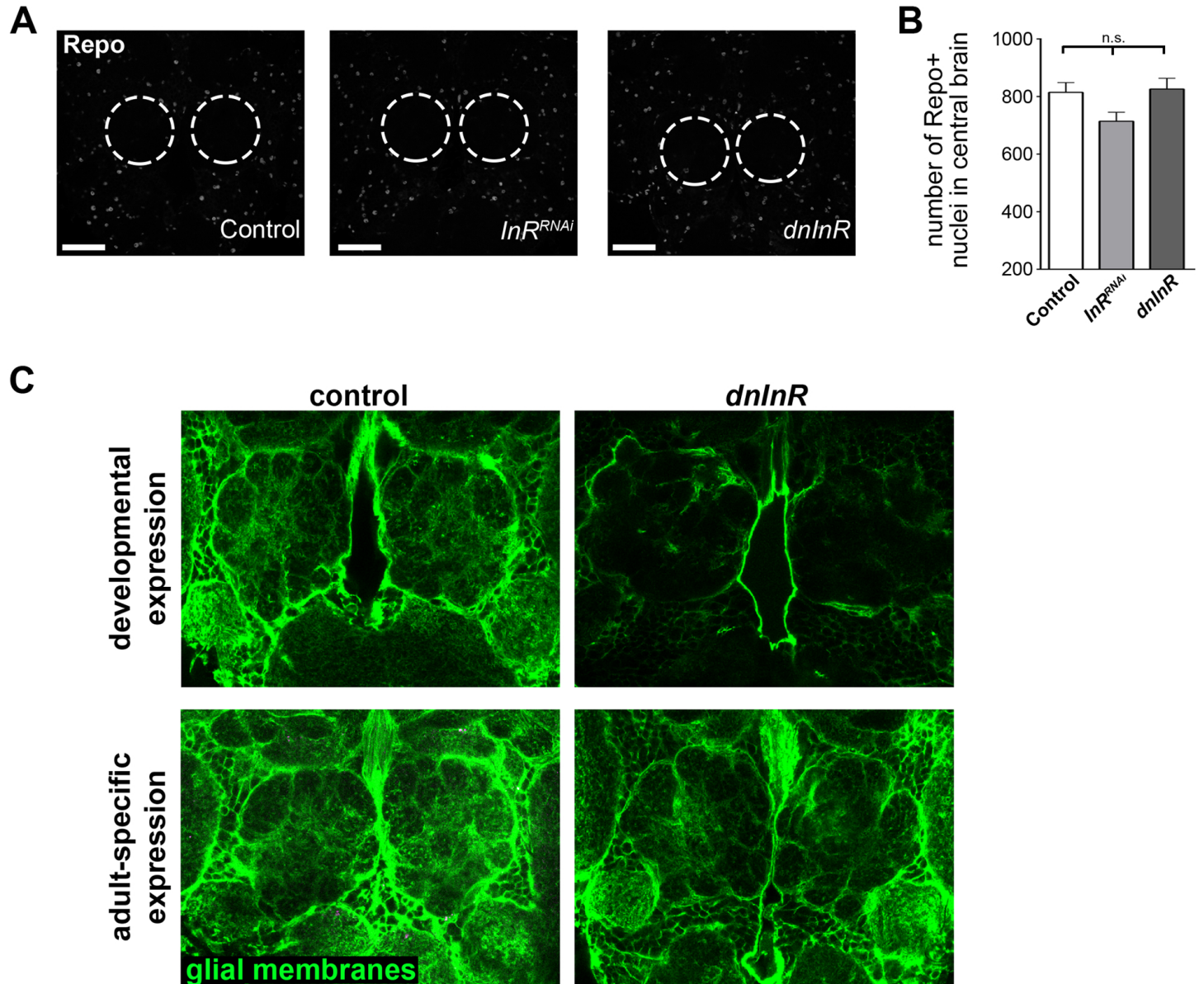


Figure S3. Related to Figure 3. Inhibition of InR in adult glia does not alter glial cell number or gross morphology. (A) Maximum intensity projections of 20 μ m Z-stack collections through central brains stained with anti-Repo. (B) Quantification of Repo+ nuclei reveals no change in glial numbers after expressing dominant negative InR or InRRNAi in adult glia for 14 days. Dotted lines denote outline of antennal lobes. $N \geq 16$ for each genotype. ns. = not significant. Scale bar: 30 μ m. Genotypes: Control (OR85e-mCD8::GFP, tub-Gal80ts/+;repo-Gal4/+), InRRNAi (OR85e-mCD8::GFP, tub-Gal80ts/+;repo-Gal4, InRex15/UAS-InRRNAi), and dnInR (OR85e-mCD8::GFP, tub-Gal80ts/+;repo-Gal4, InRex15/UAS-Dominant Negative InR). (C) Representative single confocal slice images of brains expressing repo-driven membrane-tethered GFP to show glial cell morphology. Developmental expression genotypes: control (UAS-mCD8::GFP/+; repo-Gal4, InRex15/+), dnInR (UAS-mCD8::GFP/+;repo-Gal4, InRex15/UAS-Dominant Negative InR). Adult-specific expression genotypes: control (UAS-mCD8::GFP/tub-Gal80ts; repo-Gal4, InRex15/+), dnInR (OR85e-mCD8::GFP, tub-Gal80ts/+;repo-Gal4, InRex15/UAS-Dominant Negative InR).

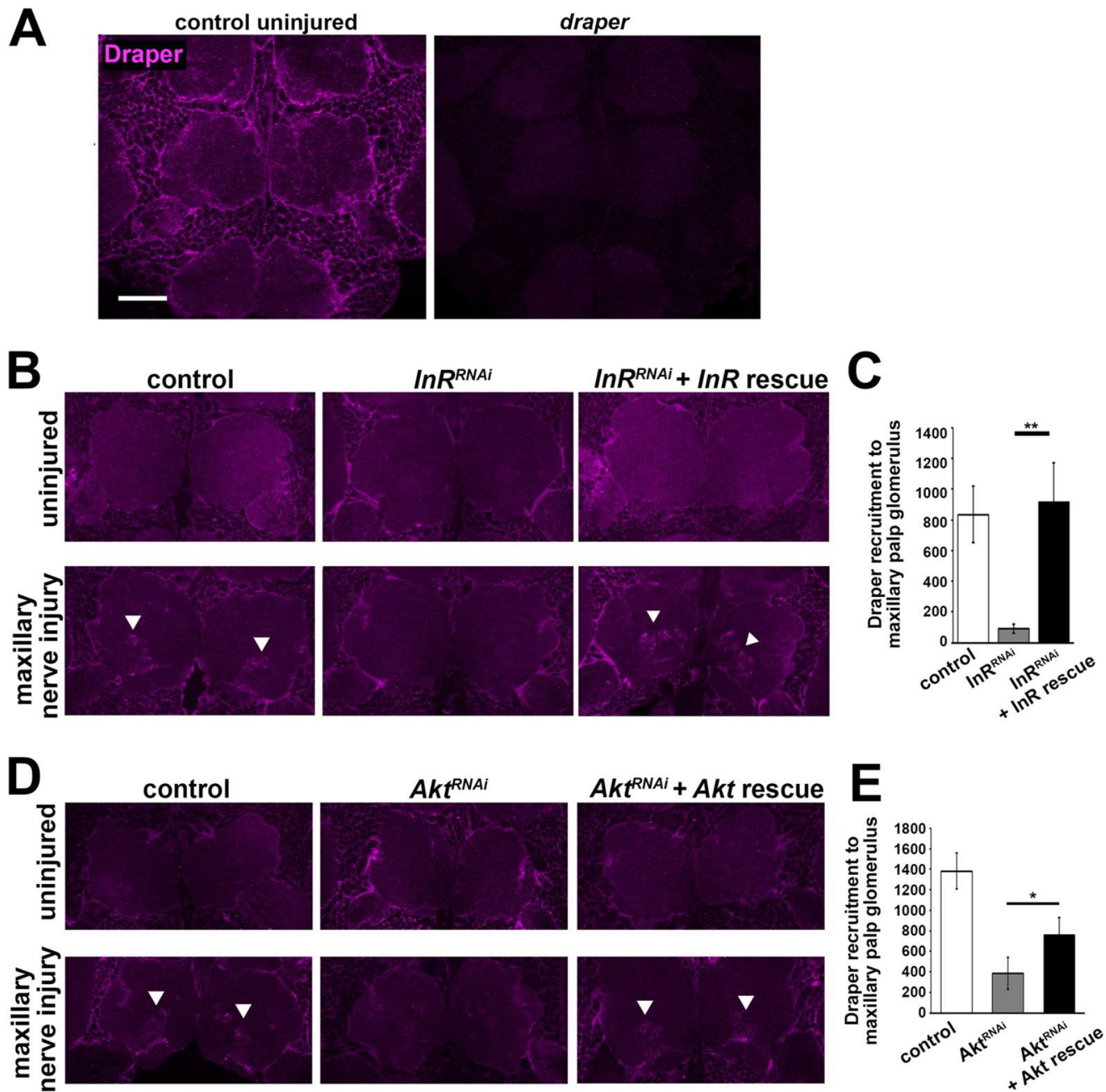


Figure S4. Related to Figure 3. Rescue of *InR*^{RNAi} and *Akt*^{RNAi} Draper recruitment phenotypes. (A) Confocal images of anti-Draper (5D14) stained brains. Genotypes: control (w1118). *draper* (*w;draperdelta5rec9*). (B) Single confocal slices of antennal lobe region of brains immunostained with anti-Draper (uninjured or 1 day after maxillary nerve axotomy). Normal Draper recruitment to injury sites (white arrowheads in control) is attenuated in glial *InR*^{RNAi} animals. Draper recruitment is restored following overexpression of the glial *InR* (*InR*^{RNAi} + *InR* rescue). (C) Quantification of Draper on OR85e maxillary palp glomeruli in B. (D) Normal Draper recruitment to injury sites (white arrowheads in control) is attenuated in glial *Akt*^{RNAi} animals. Draper recruitment is restored following overexpression of the glial *Akt* (*Akt*^{RNAi} + *Akt* rescue). (E) Quantification of Draper on OR85e maxillary palp glomeruli in D. Genotypes: control (OR85e-mCD8::GFP, tub-Gal80ts/+;repo-Gal4, *InRex15*/+). *InR*^{RNAi} (OR85e-mCD8::GFP,tub-Gal80ts/UAS-LacZ::NLS;repo-Gal4, *InRex15*/UAS-*InR*^{RNAi}). *InR*^{RNAi}+*InR* rescue (OR85e-mCD8::GFP,tub-Gal80ts/UAS-*InR*;repo-Gal4, *InRex15*/UAS-*InR*^{RNAi}). *Akt*^{RNAi} (OR85e-mCD8::GFP,tub-Gal80ts/UAS-LacZ::NLS;repo-Gal4/UAS-*Akt*^{RNAi}). *Akt*^{RNAi}+*Akt* rescue (OR85e-mCD8::GFP,tub-Gal80ts/UAS-*Akt*1;repo-Gal4/UAS-*Akt*^{RNAi}). **p*<0.05, ***p*<0.01.

SUPPLEMENTAL EXPERIMENTAL PROCEDURES

Olfactory Neuron Injuries, Dissection, and Analysis. To quantify clearance of *OR85e-mCD8::GFP* labeled debris in OR85e glomeruli, we computationally reconstructed the each *OR85e*-innervated VC6 glomerulus in entirety and performed blinded volumetric quantification of above threshold GFP⁺ fluorescent signals, with background fluorescence subtraction, using Volocity software (Perkin Elmer).

To quantify Draper recruitment to degenerating OR85e axons after maxillary nerve axotomy, we first volumetrically segmented the area of each OR85e-innervated VC6 glomerulus using GFP signal as a guide and then blindly quantified above threshold Draper⁺ fluorescent signals in this volume using Volocity. To quantify phospho-InR and phospho-Akt intensity in antennal lobe glia, we computationally segmented to the *repo-Gal4* driven *mCD8::GFP* signal (glial membranes) and then quantified total phospho-InR/Akt intensity within these GFP⁺ volumes. Phospho-InR/Akt quantification before and after antennal nerve axotomy was performed on ensheathing glial membranes located at the dorsal periphery of the antennal lobes (Figure 2A). Following maxillary nerve injury, robust accumulation of GFP⁺ glial membranes on injured maxillary nerve glomeruli can be easily identified by scrolling through collected confocal Z-stacks, which allowed us to identify volumetric boundaries for phospho-InR/Akt quantification. Volocity software (Perkin Elmer) was used to quantify Repo⁺ nuclei on 20 um stacks of the central brain region.

Antibody Use and Dilutions. The following antibodies were used at the indicated dilutions: 1:200 mouse anti-GFP (Invitrogen), 1:1000 chicken anti-GFP (Life Technologies), 1:10 mouse anti-Repo (Developmental Studies Hybridoma Bank), 1:500 mouse anti-Draper (5D14) (Abmart Inc., see below for production information), 1:500 rabbit anti-Draper (Freeman et al., 2003), 1:1000 rabbit anti-phospho-InR β (Tyr1146) (Cell Signaling), 1:2000 sheep anti- α/β Tubulin (Cytoskeleton Inc), 1:100 rabbit anti-

phospho-Drosophila Akt (Cell Signaling), 1:400 Alexa 488-conjugated donkey anti-mouse IgG (H+L) (Jackson ImmunoResearch), 1:400 Alexa Fluor 488-conjugated donkey anti-chicken IgY (H+L) (Jackson ImmunoResearch), 1:400 Rhodamine Red-X-conjugated donkey anti-mouse IgG (H+L) (Jackson ImmunoResearch), 1:400 Alexa Fluor 647-conjugated donkey anti-mouse IgG (H+L) (Jackson ImmunoResearch).

Draper Antibody Production. We generated a monoclonal mouse anti-Draper antibody against the epitope: NPIVYNESLK. This antibody was designed and produced by Abmart Inc. using their Protein Surface Epitopes Targeted by Monoclonal Antibody Library (SEAL) technique. The mouse anti-Draper antibody (supernatant 5D14 at Developmental Studies Hybridoma Bank) was used for the experiments in this manuscript. Specificity of 5D14 was confirmed on *draper* null mutant brains (Supplemental Figure 3).

Real-Time Quantitative PCR. Central brains were manually dissected central brains in Jans' saline (0.5 mM Ca²⁺) and immediately frozen on dry ice. Total RNA was extracted in Trizol reagent (Invitrogen), and the aqueous phase was isolated with a Phase Lock Gel kit (5 Prime) and the RNA passed over a RNA Clean & Concentrator-5 column (Zymo Research). RNA was treated with DNase (Ambion *DNA-free* kit), and the final RNA concentration was determined using a Qubit Fluorometer (Invitrogen). Total RNA (~25 ng) was reverse-transcribed with the qScript cDNA SuperMix kit (Quanta Biosciences) for 30 minutes at 42°C.

Quantitative PCR was performed on an Applied Biosystems StepOne Real-Time PCR System. The TaqMan Fast Advanced Master Mix kit (Applied Biosystems) and the following TaqMan assays were used: (i) Ribosomal Protein L32 (Applied Biosystems premade assay Dm02151827_g1), (ii) Draper-I custom assay: F-primer, TGTGATCATGGTTACGGAGGAC; R-primer, CAGCCGGGTGGGCAA; probe, CGCCTGCGATATAA. The 2^{-Ct} of the raw threshold cycle (C_t) of the endogenous control

(RpL32) did not significantly vary across time points and genotypes analyzed. For experimental comparisons of *draper-I* expression, statistical analysis was performed on $2^{-\Delta\Delta Ct}$ values.

RT-PCR analysis of ilp transcript expression. Third antennal segments were manually dissected from *w¹¹¹⁸* adult male and female flies. Total RNA was extracted using Trizol reagent (Invitrogen), treated with DNase (Ambion *DNA-free* kit), and the final RNA concentration was determined using a Qubit Fluorometer (Invitrogen). Total RNA was reverse-transcribed with the qScript cDNA SuperMix kit (Quanta Biosciences). The following PCR primers were used:

Gene	Sequence 5'- 3'
<i>dilp1 F</i>	ACAACGGTGCAGCAGTACAT
<i>dilp1 R</i>	AACCAATCTGTACGGATCCG
<i>dilp2 F</i>	ACCCATAACCATGAGCAAGC
<i>dilp2 R</i>	TGTGATATGAAGGCTCTGCG
<i>dilp3 F</i>	GGGATTCACGCATCCATACT
<i>dilp3 R</i>	TGCTGAGATATTGTGCTGCC
<i>dilp4 F</i>	TACCTTTTATGCCCGGTGAG
<i>dilp4 R</i>	GGAAACGGGAAGGTAAAGC
<i>dilp5 F</i>	CGTGATCCCAGTTCTCCTGT
<i>dilp5 R</i>	AAAATGCTGCGATACCTGG
<i>dilp6 F</i>	TAGTCCTGGCCACCTTGTTT
<i>dilp6 R</i>	ACTCCACCACTCCACCACTC
<i>dilp7 F</i>	GCGGAGCTGTACTCCTGTTC
<i>dilp7 R</i>	GTTTCTGCGAAGTCGTCGAT

Specificity of ilp PCR primers was confirmed using single ilp null flies as negative controls; ilp5 primers successfully amplified product from positive control larval CNS (data not shown).

Western Blots. Dissected adult brains were homogenized in 4 μ L 1xLB (Loading Buffer) per head. Protein lysate of 4-5 heads were loaded onto 4-20% Tris-Glycine gels (Lonza), transferred to PVDF membranes (Millipore), and probed with rabbit anti-Draper (1:1000) and anti-tubulin (1:2,000). Blots were incubated overnight at 4°C, washed several times with 1xPBS/0.01% Tween 20, and probed with appropriate fluorophore-conjugated antibodies secondary antibodies (Jackson ImmunoResearch) for 2 hours at room temperature. Additional washes were performed with 1xPBS/0.01% Tween 20 and a final wash in 1xPBS. Blots were imaged on G:BOX F3 Imaging System and band intensities were quantified using with the ImageJ program (Schneider et al., 2012).

RNAi screen. Flies carrying *OR85e-mCD8::GFP* and *repo-Gal4* transgenes were crosses to UAS-RNAi strains. Maxillary palp injuries were performed as described above. Three to five days after axotomy, brains were imaged by confocal microscopy and scored (non-quantitative) for defects in clearance of GFP-labeled axonal debris. RNAi lines displaying clearance defects were re-screened immunostained for Draper one day after maxillary nerve axotomy to assess Draper protein levels and Draper recruitment to injured maxillary glomeruli. See Supplemental Table 1 for list of RNAi lines.

Supplemental Table 1, Related to Figure 1. List of transgenic RNAi strains screened for glial clearance phenotype. OR85e axon clearance phenotype: “yes” indicates that GFP-labeled axonal debris persisted 3-5 days after maxillary nerve injury. Draper recruitment phenotype: “yes” indicates reduced levels of Draper visible on injured maxillary nerves 24 hours after axotomy. n/t = not tested